

Higgs boson production in association with top quarks in the POWHEG BOX

H. B. Hartanto,^{1,*} B. Jäger,^{2,†} L. Reina,^{3,‡} and D. Wackerth^{4,§}

¹*Institut für Theoretische Teilchenphysik und Kosmologie,
RWTH Aachen University, D-52056 Aachen, Germany*

²*Institute for Theoretical Physics, Tübingen University,
Auf der Morgenstelle 14, 72076 Tübingen, Germany*

³*Physics Department, Florida State University,
Tallahassee, FL 32306-4350, U.S.A.*

⁴*Department of Physics, SUNY at Buffalo, Buffalo, NY 14260-1500, U.S.A.*

(Dated: January 20, 2015)

Abstract

We present results from the analytic calculation of $t\bar{t}H$ hadronic production at Next-to-Leading Order in QCD interfaced with parton-shower Monte Carlo event generators in the POWHEG BOX framework. We consider kinematic distributions of the top quark and Higgs boson at the 8 TeV Large Hadron Collider and study the theoretical uncertainties due to specific choices of renormalization/factorization scales and parton-showering algorithms, namely PYTHIA and HERWIG. The importance of spin-correlations in the production and decay stages of a top/antitop quark is discussed on the example of kinematic distributions of leptons originating from the top/antitop decays. The corresponding code is now part of the public release of the POWHEG BOX.

*Electronic address: hartanto@physik.rwth-aachen.de

†Electronic address: barbara.jaeger@itp.uni-tuebingen.de

‡Electronic address: reina@hep.fsu.edu

§Electronic address: dow@ubpheno.physics.buffalo.edu

I. INTRODUCTION

The associated production of a Higgs boson with a pair of top (t) and antitop quarks (\bar{t}) has been receiving increased attention after the discovery of a Higgs boson (H) at the CERN Large Hadron Collider (LHC) [1, 2]. Although rare in nature, this production mode gives direct access to the Higgs-boson coupling to the heaviest elementary fermion, the top quark, and provides important constraints on extensions of the Standard Model (SM) when combined with the indirect determination of the same coupling in Higgs-boson production via loop-induced gluon-gluon fusion. Experimental studies of Higgs properties have already provided strong constraints in Run 1 [3–5], and will be one of the main focuses of Run 2 of the LHC.

Recent experimental analyses have explored the possibility of detecting $t\bar{t}H$ production when the Higgs boson decays via $H \rightarrow b\bar{b}$ [6–9], $H \rightarrow \gamma\gamma$ [10–12], and $H \rightarrow ZZ^*, WW^*$ [13], or in a combination of all the previous modes [14]. Apart from overcoming challenging background difficulties, it is important first of all to have the signal fully under control, including the decay of the final-state particles. With this respect, the theoretical systematic error has to be carefully investigated and reduced, if possible, by adding both QCD and electroweak higher-order corrections consistently interfaced with existing parton-shower (PS) Monte Carlo codes, e.g. `PYTHIA` [15, 16], `HERWIG` [17, 18] or `SHERPA` [19], to match the complexity of real events.

The parton-level $\mathcal{O}(\alpha_s^3)$ or next-to-leading order (NLO) QCD cross section for $t\bar{t}H$ production has been first calculated in Refs. [20–25] and subsequently confirmed by various collaborations using one-loop computational tools such as `aMC@NLO` [26, 27] and `PowHe1` [28, 29]. More recently the $\mathcal{O}(\alpha_s\alpha^2)$ contribution to the parton level cross section has also been calculated including [30] or omitting [31] QED corrections. Effects of parton shower and hadronization on the NLO-QCD parton-level cross sections have been studied both in the `aMC@NLO` framework [26] and in a private implementation of the `POWHEG` method by the `PowHe1` collaboration [28]. The two approaches have been compared and found in good agreement in a study performed within the LHC Higgs Cross Section Working Group [32]. More recently, the original NLO-QCD calculation of Refs. [22–25] has been interfaced with `SHERPA` [19] and has become part of the `SHERPA-2.0.0` release. We have now interfaced the same routines with the `POWHEG BOX` [33–35] including the decays of the top/antitop quarks

and the Higgs boson. The top-quark spin-correlations have been taken into account in an approximate way, similar to what has been done in the `aMC@NLO` [36] and `PowHel` [28] implementations, to allow for studies based on top-quark spin-polarization effects [36–38]. A first comparison of this interface with `PowHel` and `SHERPA`, that did not include spin-correlation effects, was presented in the context of the Les Houches 2013 Workshop [39]. After more detailed cross checks and further improvements, we are now making our implementation public through the `POWHEG BOX` website, <http://powhegbox.mib.infn.it/>.

In view of the dedicated effort on $t\bar{t}H$ analyses in both the ATLAS and CMS collaborations, in this paper we would like to present the details of our implementation and take the opportunity to address some of the issues that have emerged in recent experimental studies. In particular, we will investigate the dependence of theoretical predictions on the choice of a static or dynamical renormalization/factorization scale, the possibly different behavior of the interface with `PYTHIA/HERWIG`, and the effect of top-quark spin-correlations on various kinematic distributions of the decay products of the $t\bar{t}H$ final state. Even though the background to $t\bar{t}H$ represents a major hurdle which needs to be overcome in order to properly measure this very important production channel, a very accurate control of the signal is still the first necessary step, and the possibility for the experimental community to have access to several public tools is very valuable. Our implementation answers this need and provides the original NLO-QCD analytic calculation [22–25] in the same framework (`POWHEG BOX` in this case) as other processes that enter the $t\bar{t}H$ studies, from $t\bar{t}$ production [40] to single-top production [41] or Higgs production in gluon-gluon fusion [42, 43], offering a fully consistent alternative to analogous studies in the `MadGraph5_aMC@NLO` [44] framework.

II. IMPLEMENTATION

The implementation of a new process in the framework of the `POWHEG BOX` requires a list of all independent flavor structures for the Born and the real-emission contributions, the Born and the real-emission amplitudes squared, the finite parts of the virtual amplitudes interfered with the Born amplitude, the spin- and color correlated amplitudes squared, and a parametrization of the phase space for the Born process. The tree-level amplitudes can be generated with the help of the build tool based on `MadGraph 4` [45, 46] that is available in the `POWHEG BOX`. For $pp \rightarrow t\bar{t}H$, we use the virtual amplitudes of [22–25] and adapt them

to the format required by the POWHEG BOX. In order to validate our implementation, we have checked that the results of [24, 25] are fully reproduced by the NLO-QCD mode of the POWHEG BOX.

The fixed-order calculation of [22–25] provides NLO-QCD corrections to the production of an on-shell $t\bar{t}H$ state at a hadron collider. If implemented in a multi-purpose Monte-Carlo program like PYTHIA, decays of the scalar Higgs boson can easily be simulated. In principle, also the decays of the top quarks can be taken care of externally. However, merely combining the on-shell calculation for $pp \rightarrow t\bar{t}H$ with a separate, spin-averaged simulation of the top-quark decays by the shower Monte Carlo results in a loss of information on correlations between the production and the decay stages.

A method for overcoming this limitation was proposed in [47] and has by now been applied in several POWHEG BOX implementations of processes with unstable particles [41, 48, 49]. The basic idea of this approach is to first produce on-shell $t\bar{t}H$ events including NLO-QCD corrections matched to a parton-shower generator (NLO+PS) via the POWHEG framework, and subsequently simulate the decays according to a distribution determined by matrix elements for $H(t \rightarrow b\ell^+\nu)(\bar{t} \rightarrow \bar{b}\ell^-\bar{\nu})$ and $H(t \rightarrow b\ell^+\nu)(\bar{t} \rightarrow \bar{b}\ell^-\bar{\nu}) + \text{jet}$ final states that retain correlations in the top-quark decays, both at leading order and in the real-emission contributions. In addition to an improved description of spin correlations between the production and decay stages, this method allows for a moderate reshuffling of momenta in such a way that the virtualities of the top quarks are distributed according to Breit-Wigner shapes. For the actual implementation of this procedure we follow closely what has been done for the related case of $t\bar{t} + \text{jet}$ production [49], and refer the reader to that reference for further technical details. The code version we are providing in the POWHEG BOX allows the user to activate this feature for an improved description of top-quark decays via a switch in the input file. Alternatively, the code can generate on-shell events for $pp \rightarrow t\bar{t}H$ that are subsequently decayed externally, for instance via PYTHIA.

III. RESULTS

The results presented in this section have been obtained using a prototype setup where we consider the LHC operating at $\sqrt{s} = 8$ TeV, with the top quark and Higgs boson masses chosen to be, respectively, $m_t = 172.5$ GeV, and $m_H = 125$ GeV. After having validated

the POWHEG BOX implementation against the parton-level NLO-QCD results of Refs. [22–25], we have focused on some of the issues that have been raised in recent experimental analyses concerning differences encountered in the behavior of several distributions when interfacing the NLO-QCD calculation of $pp \rightarrow t\bar{t}H$ with either PYTHIA or HERWIG. With this respect, results are presented using the PYTHIA-6.4.25 [15], PYTHIA-8.183 [16], and HERWIG-6.5.10 [18] releases of the aforementioned parton-shower algorithms. We note that, in principle, POWHEG requires a transverse-momentum ordered parton-shower program, such as PYTHIA. In order to correct for unwanted radiation effects that occur in angular-ordered parton shower programs, such as HERWIG, a vetoed-truncated shower has to be included. Since the public version of HERWIG does not provide a truncated shower, we neglect these contributions and consider them as part of the systematic uncertainties of our results. In all our numerical results, underlying event and multi-parton interactions are disregarded. We note that more specific studies should be developed in the context of dedicated experimental analyses and we facilitate them by making our codes public through the POWHEG BOX.

In this section we choose to illustrate the reach of our implementations by showing a sample of distributions for the main final-state objects (t , \bar{t} , and H) and their decay products, obtained by interfacing the NLO-QCD calculation with both PYTHIA and HERWIG. Indeed for our numerical analysis, we only consider the decay products of the top and antitop quarks. Decays of the scalar Higgs boson (no spin-correlation involved) can easily be simulated with the external parton-shower Monte Carlo, and we provide a respective option in the public version of our POWHEG BOX implementation. We study the dependence of distributions on the choice of either a fixed or a dynamical renormalization/factorization scale. We do not take up a study of other issues, like the dependence on intrinsic parton-shower scales, or the residual uncertainty due to the choice of Parton Distribution Functions (PDF). These studies are important and should be performed in the context of specific experimental analyses. All our results are presented using the CT10nlo [50] set of PDF as implemented in the LHAPDF library [51] with the number of light quark flavors set to $N_f = 5$ and the strong coupling at NLO QCD determined by $\alpha_s(M_Z) = 0.118$.

To explore the issue of scale dependence, we set the renormalization and factorization scales equal to each other and studied both the case of a fixed and a dynamical scale. When using a fixed scale we have chosen $\mu_0 = m_t + m_H/2$ as central scale, while we have chosen $\mu_0 = (m_T(t)m_T(\bar{t})m_T(H))^{1/3}$ as central value when working with a dynamical scale (where

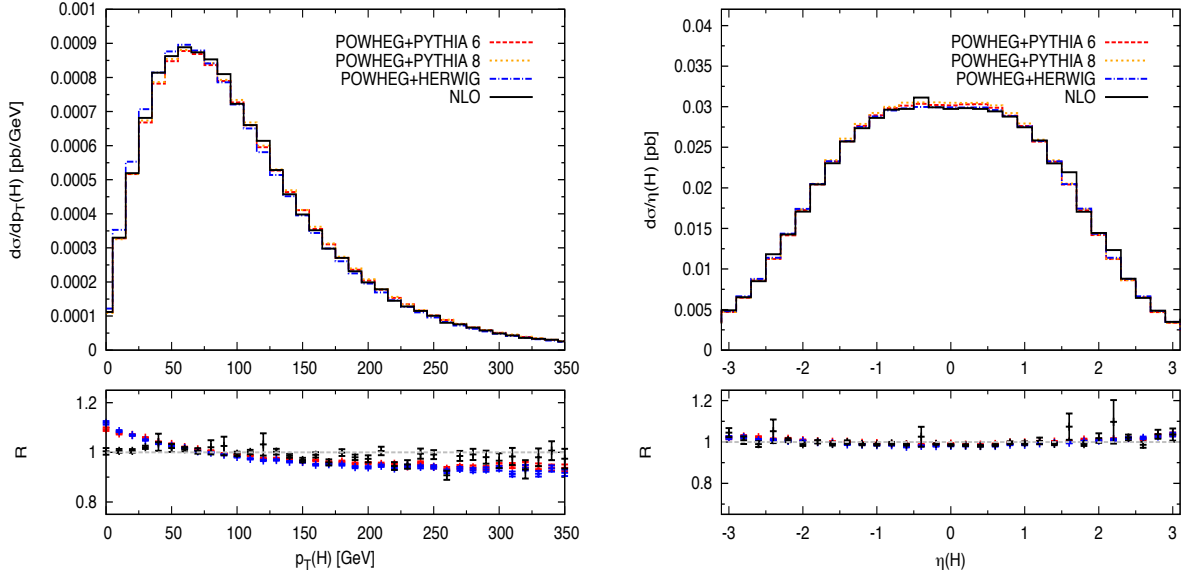


FIG. 1: The p_T (left) and η (right) distributions of the Higgs boson at NLO-QCD with no parton shower (solid, black), and with parton shower as obtained through POWHEG+PYTHIA6 (long-dashed, red), POWHEG+PYTHIA8 (short-dashed, orange), and POWHEG+HERWIG (dot-dashed, blue) respectively, for a fixed-scale choice (see text). The lower panels show the ratios: $R = d\sigma(\text{NLO})/d\sigma(\text{PYTHIA6})$ (black), $R = d\sigma(\text{HERWIG})/d\sigma(\text{PYTHIA6})$ (red), and $R = d\sigma(\text{HERWIG})/d\sigma(\text{PYTHIA8})$ (blue). The error bars indicate the statistical uncertainties of the Monte-Carlo integration.

$m_T(P)$ denotes the transverse mass of particle P). The renormalization/factorization scale dependence of the results is assessed by arbitrarily varying such scales by factors of $\xi = 1/2$ and 2 about the central value μ_0 . As default choice, we opt for the fixed scale and use $\mu_R = \mu_F = m_t + m_H/2$ unless otherwise specified.

To study the impact of different parton-shower generators on the NLO-QCD parton-level results, we present in Figs. 1-3 the comparison between the parton-level NLO-QCD results and the corresponding results obtained upon matching with either PYTHIA6, PYTHIA8, or HERWIG as implemented in the POWHEG BOX framework. In Figs. 1-2 we illustrate the impact of the parton shower on the fixed-order NLO-QCD results for the transverse-momentum and rapidity distributions of the Higgs boson and the top quark, respectively. Parton-shower effects do not cause large changes compared to the NLO results of these distributions, and differences between the PYTHIA and the HERWIG implementations are small. We noticed

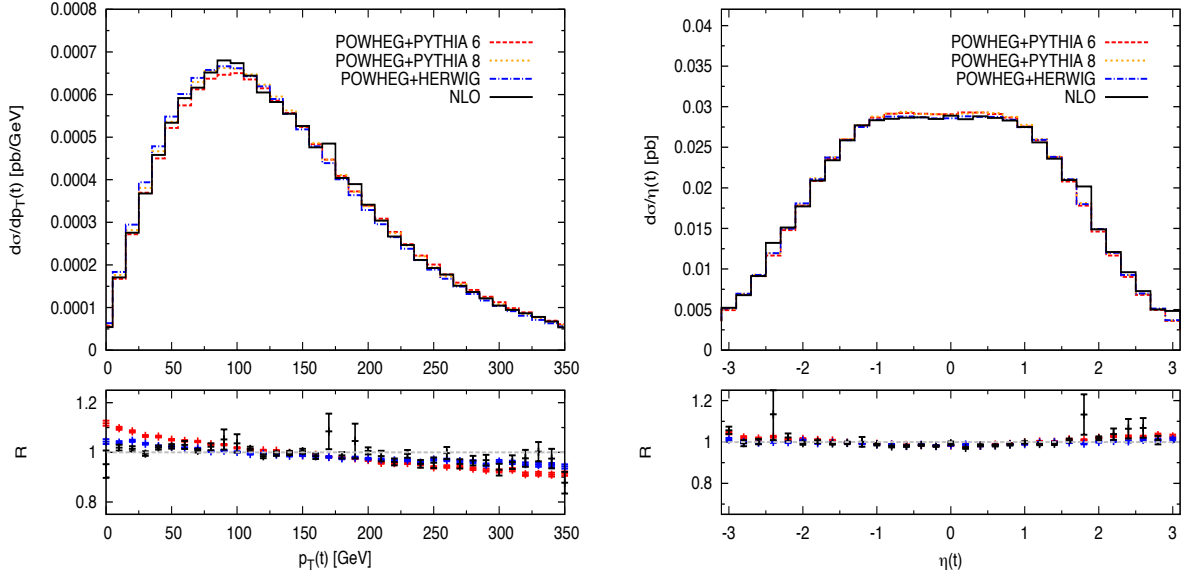


FIG. 2: The p_T (left) and η (right) distributions of the top quark at NLO-QCD with no parton shower (solid, black), and with parton shower as obtained through POWHEG+PYTHIA6 (long-dashed, red), POWHEG+PYTHIA8 (short-dashed, orange), and POWHEG+HERWIG (dot-dashed, blue) respectively, for a fixed-scale choice (see text). The lower panels show the ratios: $R = d\sigma(\text{NLO})/d\sigma(\text{PYTHIA6})$ (black), $R = d\sigma(\text{HERWIG})/d\sigma(\text{PYTHIA6})$ (red), and $R = d\sigma(\text{HERWIG})/d\sigma(\text{PYTHIA8})$ (blue). The error bars indicate the statistical uncertainties of the Monte-Carlo integration.

however a systematic enhancement of the low p_T region in HERWIG with respect to PYTHIA6, while PYTHIA8 seems to have a better agreement with HERWIG over the entire p_T spectrum. The right panel of Fig. 3 shows the transverse momentum of the $t\bar{t}H$ system. This observable is entirely due to real-radiation contributions in the NLO-QCD corrections and parton-shower effects. At leading order, the transverse momentum of the $t\bar{t}H$ system is zero, because of momentum conservation. If real-emission contributions are taken into account, as in the fixed-order NLO-QCD calculation, this observable exhibits a divergence as the transverse momentum of the entire system approaches zero. In the NLO+PS result, this behavior is tamed by a Sudakov factor. The POWHEG+PYTHIA and POWHEG+HERWIG results are thus much better behaved in the region of low $p_T(t\bar{t}H)$ that correspond to the emission of a soft jet, and they are compatible over the full p_T spectrum. We could present distributions for jet observables as well, starting from the p_T and η of the hardest or next-to-hardest jets,

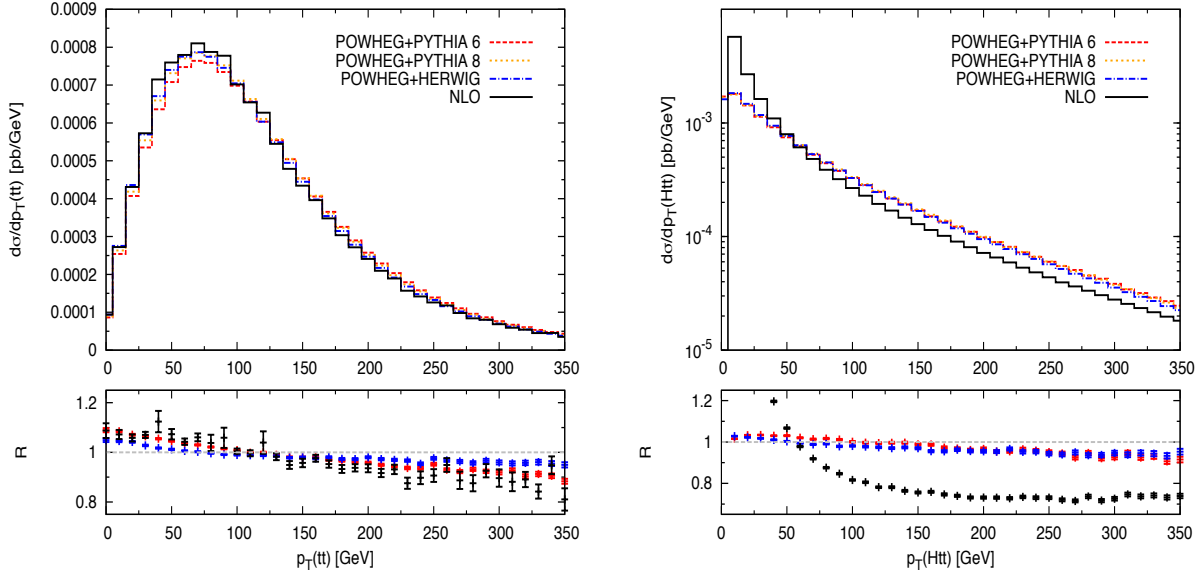


FIG. 3: The p_T distributions of the $t\bar{t}$ pair (left) and of the $t\bar{t}H$ system (right) at NLO-QCD with no parton shower (solid, black), and with parton shower as obtained through POWHEG+PYTHIA6 (long-dashed, red), POWHEG+PYTHIA8 (short-dashed, orange), and POWHEG+HERWIG (dot-dashed, blue) respectively, for a fixed-scale choice (see text). The lower panels show the ratios: $R = d\sigma(\text{NLO})/d\sigma(\text{PYTHIA6})$ (black), $R = d\sigma(\text{HERWIG})/d\sigma(\text{PYTHIA6})$ (red), and $R = d\sigma(\text{HERWIG})/d\sigma(\text{PYTHIA8})$ (blue). The error bars indicate the statistical uncertainties of the Monte-Carlo integration.

but they would not help us to judge the impact of the parton shower if we did not set in place, at the same time, more specific selection cuts aimed at distinguishing the first emission described by the hard matrix elements or the top-quark decays from the following emissions coming from the parton shower, as well as cuts and vetoes aimed at distinguishing light jets from heavy-flavor jets. Since these sort of requirements only make sense in the context of dedicated experimental analyses, we refrain from considering specific jet variables and present only results for observables of systems, like the $t\bar{t}H$ system, that carry a clear imprint of the jet from the first QCD emission, and allow us to verify expected effects like the one due to the Sudakov factor.

In order to assess the theoretical uncertainties associated with the choice of renormalization and factorization scale, we have computed the previously considered distributions for different choices of scale as previously explained. In particular, Figs. 4-6 are obtained using

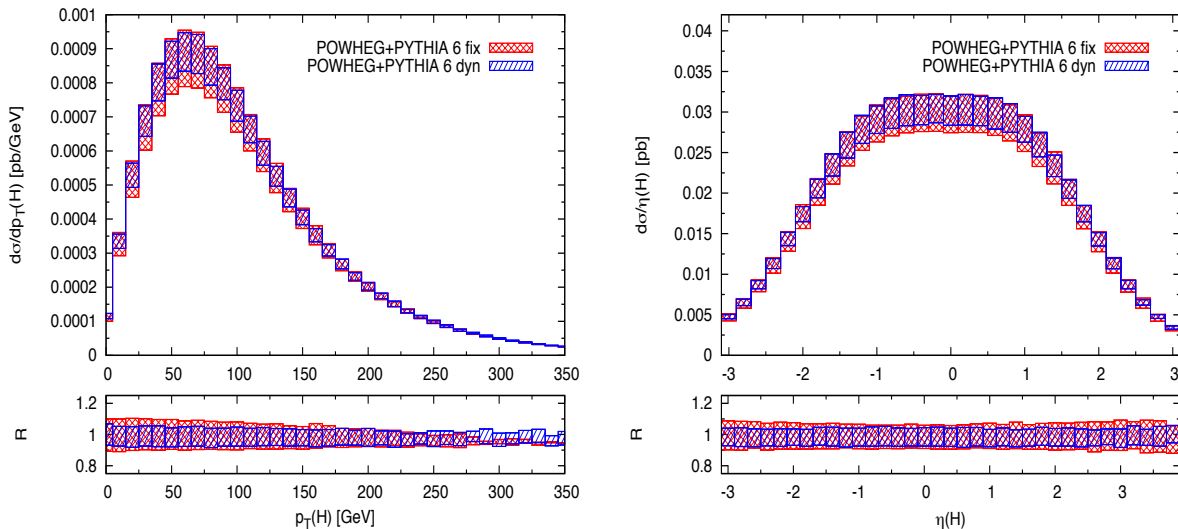


FIG. 4: The p_T (left) and η (right) distributions of the Higgs boson obtained with POWHEG+PYTHIA6 for fixed (*fix*) and dynamical (*dyn*) renormalization/factorization scales. The lower panels show the respective ratios $R = d\sigma(\xi\mu_0)/d\sigma(\mu_0)$ for $\xi = (0.5; 2)$.

our POWHEG+PYTHIA6 implementation. More specifically, Figs. 4 and 5 show the transverse momentum and rapidity distributions of the Higgs boson and the top quark, respectively. The scale dependence of the results is considerable, amounting to more than $\pm 10\%$ in some regions of phase space. Using a dynamical rather than a fixed scale helps in slightly reducing the scale uncertainty of the NLO+PS results in all observables.

A similar behavior can be observed in the transverse momentum distributions of the $t\bar{t}$ pair and the $t\bar{t}H$ system, c.f. Fig. 6. Since the latter observable vanishes at leading order, we expect it to be plagued by larger uncertainties than distributions that are genuinely described at NLO accuracy.

We finally illustrate the impact of spin-correlation effects. As pointed out, for instance in Ref. [38], exploiting polarization effects in the top-quark decays can appreciably improve the sensitivity of the LHC in the $t\bar{t}H$ channel. At the same time, spin-correlation observables can probe the top-Higgs coupling in $t\bar{t}H$ production at the LHC, as studied for instance in Ref. [52]. To allow for the simulation of spin correlations in the decays of the top quarks our POWHEG BOX implementation resorts to the prescription of Ref. [47], as explained in Sec. II. NLO-QCD corrections are considered for the $t\bar{t}H$ production process only. Improving on

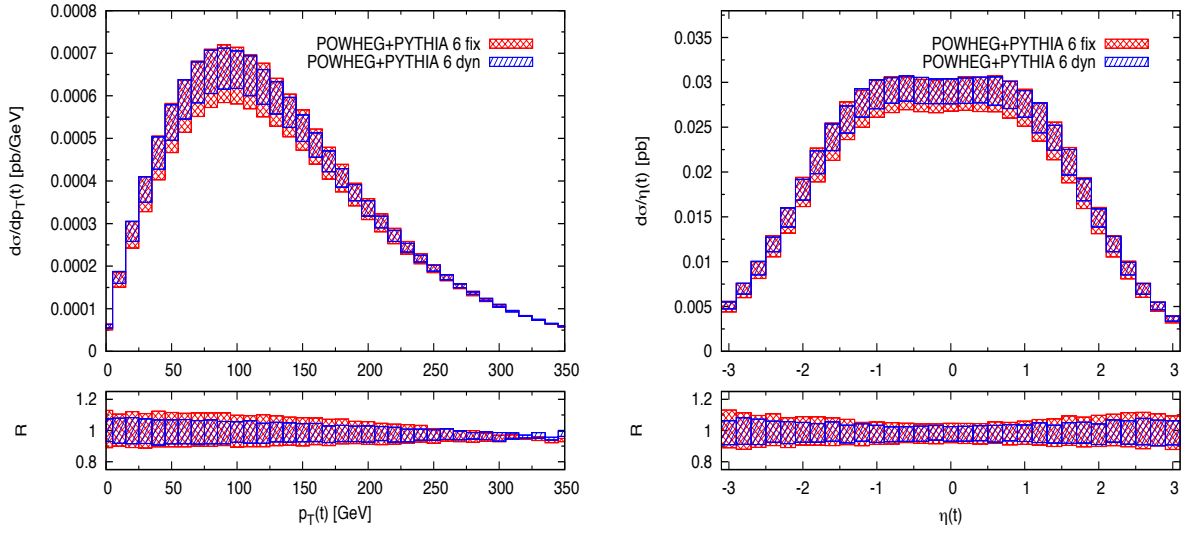


FIG. 5: The p_T (left) and η (right) distributions of the top quark obtained with POWHEG+PYTHIA6 for fixed (*fix*) and dynamical (*dyn*) renormalization/factorization scales. The lower panels show the respective ratios $R = d\sigma(\xi\mu_0)/d\sigma(\mu_0)$ for $\xi = (0.5; 2)$.

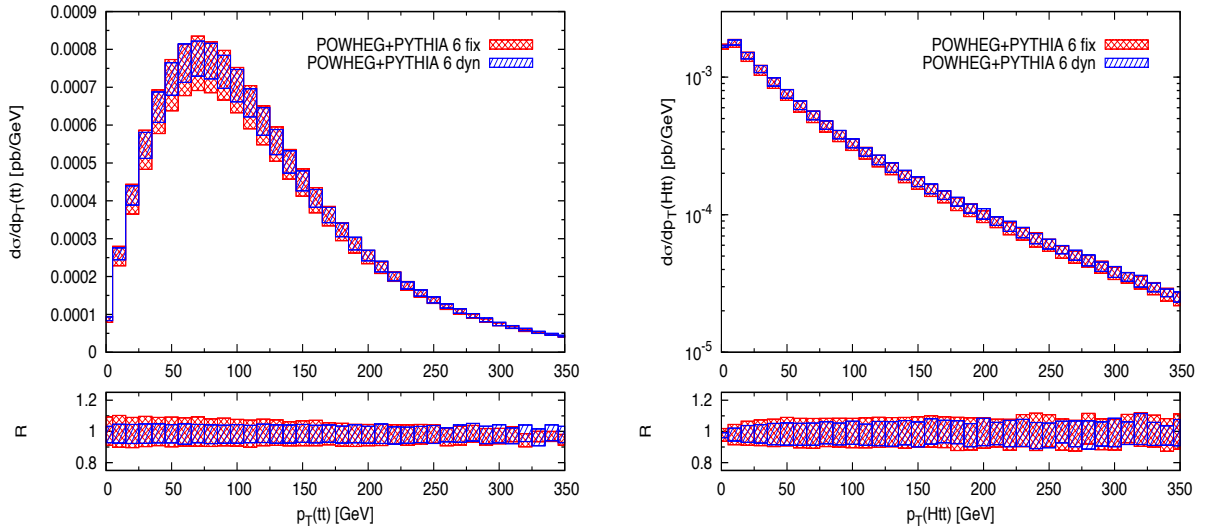


FIG. 6: The p_T distributions of the $t\bar{t}$ pair (left) and of the $t\bar{t}H$ system (right) obtained with POWHEG+PYTHIA6 for fixed (*fix*) and dynamic (*dyn*) renormalization/factorization scales. The lower panels show the respective ratios $R = d\sigma(\xi\mu_0)/d\sigma(\mu_0)$ for $\xi = (0.5; 2)$.

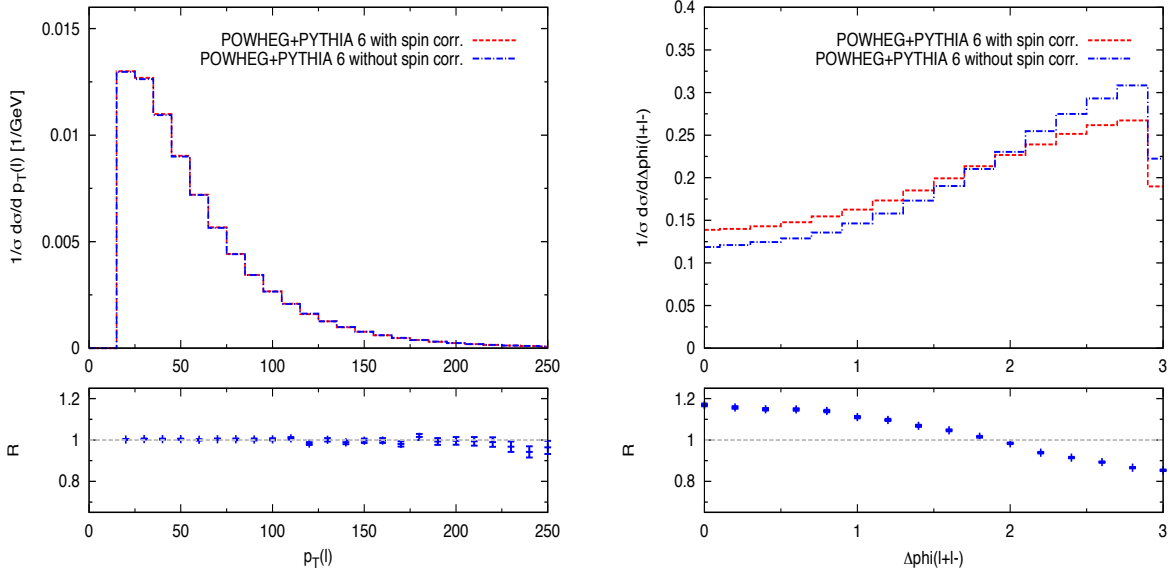


FIG. 7: Normalized transverse-momentum distribution of the hardest lepton (left) and azimuthal angle separation of the two hardest oppositely charged leptons (right) obtained with POWHEG+PYTHIA6 with (blue lines) and without (red lines) spin correlations in the decays of the top quarks, for a dynamic-scale choice (see text). The lower panels show the ratios of the results without and with spin correlations.

the accuracy of the decay process would require more advanced techniques, such as the method that has recently been presented for top quark pair production at the LHC [53]. For processes with additional particles in the final state, such as $t\bar{t}H$ production, such a procedure has never been applied so far and we restrict ourselves to the more approximated description of the decay process for the time being. To explore the impact of spin-correlation effects on experimentally accessible observables, we consider the leptonic decay modes of the top quarks and focus on final states with at least two oppositely charged leptons with

$$p_{T,\ell} > 20 \text{ GeV}, \quad |y_\ell| < 2.5, \quad (1)$$

that are well-separated by $\Delta R_{\ell,j} > 0.4$ from identified jets with $p_{T,j} > 20 \text{ GeV}$ and $|y_j| < 4.5$. As illustrated by Fig. 7, the transverse-momentum distribution of a hard lepton barely depends on the treatment of the top-quark decays. Predictions for angular correlations between the two hardest oppositely-charged leptons, however, exhibit a sizable modification when the simulation of the top-quark decays is improved.

IV. CONCLUSIONS

In this work we have presented a new, public implementation of $t\bar{t}H$ production at the LHC at NLO-QCD matched to parton showers in the framework of the POWHEG BOX. In order to illustrate the reach of the implementation, we discussed several sources of theoretical uncertainties, in particular scale dependencies and differences due to the specific shower Monte Carlo program used. We found that, within the limits of such a general study, for most observables differences between predictions obtained with PYTHIA6, with PYTHIA8, and with HERWIG are small. We remind the reader that the public version of HERWIG that we have used does not have any vetoed truncated showers and therefore the comparison between PYTHIA and HERWIG will have to be further investigated in particular in analyses that include jet observables. Scale uncertainties are generally non-negligible and can amount to more than $\pm 10\%$ in some regions of phase space. The uncertainties obtained using a dynamical and a fixed scale are compatible, although typically they are smaller when using a dynamical scale. For observables involving the decay products of the top quark, we recommend using a code version that does take into account spin correlations between the production and decay stages.

Acknowledgements

We are grateful to Carlo Oleari for his assistance in making this code publicly available on the POWHEG BOX website. This work was supported in part by the National Science Foundation under Grant No. PHYS-1066293 and the Aspen Center for Physics. The work of B. J. is supported in part by the Institutional Strategy of the University of Tübingen (DFG, ZUK 63). The work of L. R. is supported in part by the U.S. Department of Energy under grant DE-FG02-13ER41942. The work of D. W. is supported in part by the U.S. National Science Foundation under award no. PHY-1118138.

-
- [1] G. Aad et al. (ATLAS Collaboration), Phys.Lett. **B716**, 1 (2012), 1207.7214.
 - [2] S. Chatrchyan et al. (CMS Collaboration), Phys.Lett. **B716**, 30 (2012), 1207.7235.
 - [3] S. Chatrchyan et al. (CMS Collaboration), Phys.Rev.Lett. **110**, 081803 (2013), 1212.6639.

- [4] G. Aad et al. (ATLAS Collaboration), Phys.Lett. **B726**, 120 (2013), 1307.1432.
- [5] ATLAS Collaboration (2013), ATLAS-CONF-2013-034, ATLAS-COM-CONF-2013-035.
- [6] ATLAS Collaboration (2012), ATLAS-CONF-2012-135, ATLAS-COM-CONF-2012-162.
- [7] CMS Collaboration (2012), CMS-PAS-HIG-12-025.
- [8] S. Chatrchyan et al. (CMS Collaboration), JHEP **1305**, 145 (2013), 1303.0763.
- [9] ATLAS collaboration (2014), ATLAS-CONF-2014-011, ATLAS-COM-CONF-2014-004.
- [10] ATLAS collaboration (2013), ATLAS-CONF-2013-080, ATLAS-COM-CONF-2013-089.
- [11] CMS Collaboration (2013), CMS-PAS-HIG-13-015.
- [12] ATLAS collaboration (2014), ATLAS-CONF-2014-043, ATLAS-COM-CONF-2014-059.
- [13] CMS Collaboration (2013), CMS-PAS-HIG-13-020.
- [14] V. Khachatryan et al. (CMS Collaboration), JHEP **1409**, 087 (2014), 1408.1682.
- [15] T. Sjostrand, S. Mrenna, and P. Z. Skands, JHEP **0605**, 026 (2006), hep-ph/0603175.
- [16] T. Sjostrand, S. Mrenna, and P. Z. Skands, Comput.Phys.Commun. **178**, 852 (2008), 0710.3820.
- [17] G. Marchesini, B. Webber, G. Abbiendi, I. Knowles, M. Seymour, et al., Comput.Phys.Commun. **67**, 465 (1992).
- [18] G. Corcella, I. Knowles, G. Marchesini, S. Moretti, K. Odagiri, et al., JHEP **0101**, 010 (2001), hep-ph/0011363.
- [19] T. Gleisberg, S. Hoeche, F. Krauss, M. Schonherr, S. Schumann, et al., JHEP **0902**, 007 (2009), 0811.4622.
- [20] W. Beenakker et al., Phys. Rev. Lett. **87**, 201805 (2001), hep-ph/0107081.
- [21] W. Beenakker et al., Nucl. Phys. **B653**, 151 (2003), hep-ph/0211352.
- [22] L. Reina and S. Dawson, Phys. Rev. Lett. **87**, 201804 (2001), hep-ph/0107101.
- [23] L. Reina, S. Dawson, and D. Wackerath, Phys.Rev. **D65**, 053017 (2002), hep-ph/0109066.
- [24] S. Dawson, L. H. Orr, L. Reina, and D. Wackerath, Phys. Rev. **D67**, 071503 (2003), hep-ph/0211438.
- [25] S. Dawson, C. Jackson, L. Orr, L. Reina, and D. Wackerath, Phys.Rev. **D68**, 034022 (2003), hep-ph/0305087.
- [26] R. Frederix et al., Phys. Lett. **B701**, 427 (2011), 1104.5613.
- [27] V. Hirschi et al., JHEP **05**, 044 (2011), 1103.0621.
- [28] M. Garzelli, A. Kardos, C. Papadopoulos, and Z. Trocsanyi, Europhys.Lett. **96**, 11001 (2011),

- 1108.0387.
- [29] G. Bevilacqua et al. (2011), 1110.1499.
 - [30] Y. Zhang, W.-G. Ma, R.-Y. Zhang, C. Chen, and L. Guo, Phys.Lett. **B738**, 1 (2014), 1407.1110.
 - [31] S. Frixione, V. Hirschi, D. Pagani, H. Shao, and M. Zaro, JHEP **1409**, 065 (2014), 1407.0823.
 - [32] S. Dittmaier, S. Dittmaier, C. Mariotti, G. Passarino, R. Tanaka, et al. (2012), 1201.3084.
 - [33] P. Nason, JHEP **0411**, 040 (2004), hep-ph/0409146.
 - [34] S. Frixione, P. Nason, and C. Oleari, JHEP **0711**, 070 (2007), 0709.2092.
 - [35] S. Alioli, P. Nason, C. Oleari, and E. Re, JHEP **1006**, 043 (2010), 1002.2581.
 - [36] P. Artoisenet, R. Frederix, O. Mattelaer, and R. Rietkerk, JHEP **1303**, 015 (2013), 1212.3460.
 - [37] F. Demartin, F. Maltoni, K. Mawatari, B. Page, and M. Zaro, Eur.Phys.J. **C74**, 3065 (2014), 1407.5089.
 - [38] S. Biswas, R. Frederix, E. Gabrielli, and B. Mele, JHEP **1407**, 020 (2014), 1403.1790.
 - [39] J. Butterworth, G. Dissertori, S. Dittmaier, D. de Florian, N. Glover, et al. (2014), 1405.1067.
 - [40] S. Frixione, P. Nason, and G. Ridolfi, JHEP **0709**, 126 (2007), 0707.3088.
 - [41] S. Alioli, P. Nason, C. Oleari, and E. Re, JHEP **0909**, 111 (2009), 0907.4076.
 - [42] S. Alioli, P. Nason, C. Oleari, and E. Re, JHEP **0904**, 002 (2009), 0812.0578.
 - [43] E. Bagnaschi, G. Degrossi, P. Slavich, and A. Vicini, JHEP **1202**, 088 (2012), 1111.2854.
 - [44] J. Alwall, R. Frederix, S. Frixione, V. Hirschi, F. Maltoni, et al., JHEP **1407**, 079 (2014), 1405.0301.
 - [45] T. Stelzer and W. Long, Comput.Phys.Commun. **81**, 357 (1994), hep-ph/9401258.
 - [46] J. Alwall, P. Demin, S. de Visscher, R. Frederix, M. Herquet, et al., JHEP **0709**, 028 (2007), 0706.2334.
 - [47] S. Frixione, E. Laenen, P. Motylinski, and B. R. Webber, JHEP **0704**, 081 (2007), hep-ph/0702198.
 - [48] C. Oleari and L. Reina, JHEP **1108**, 061 (2011), 1105.4488.
 - [49] S. Alioli, S.-O. Moch, and P. Uwer, JHEP **1201**, 137 (2012), 1110.5251.
 - [50] H.-L. Lai, M. Guzzi, J. Huston, Z. Li, P. M. Nadolsky, et al., Phys.Rev. **D82**, 074024 (2010), 1007.2241.
 - [51] M. Whalley, D. Bourilkov, and R. Group (2005), hep-ph/0508110.
 - [52] F. Boudjema, R. M. Godbole, D. Guadagnoli, and K. A. Mohan (2015), 1501.03157.

[53] J. M. Campbell, R. K. Ellis, P. Nason, and E. Re (2014), 1412.1828.